Journal of Organometallic Chemistry 886 (2019) 57–64

Contents lists available at ScienceDirect

Journal of Organometallic Chemistry

journal homepage: www.elsevier.com/locate/jorganchem

Palladium-melamine complex anchored on magnetic nanoparticles: A novel promoter for C-C cross coupling reaction

Mohammad Ali Bodaghifard [a, b, *]

[a] Department of Chemistry, Faculty of Science, Arak University, 38156-88349, Arak, Iran
[b] Institute of Nanosciences & Nanotechnology, Arak University, Arak, Iran

ARTICLE INFO

Article history:
Received 27 October 2018
Received in revised form
24 January 2019
Accepted 6 February 2019
Available online 8 February 2019

Keywords:
Palladium
Nanocatalyst
Magnetic separation
Heck reaction
Magnetic nanoparticles

ABSTRACT

A palladium-melamine complex deposited on Fe_3O_4@SiO_2 nanoparticles (MNPs-Mel-Pd) was considered as an effective catalyst for C-C cross-coupling (Mirozoki-Heck) reaction. Surface and magnetic properties of the prepared core-shell hybrid nanocatalyst was characterized using Fourier transform infrared spectroscopy, X-ray diffraction, thermogravimetric analysis, energy-dispersive X-ray, vibrating sample magnetometry, transmission and scanning electron microscopy techniques and ICP/OES analysis. It was found that the heterogeneous nanocatalyst could be recovered simply and reused numerous times without loss of its catalytic activity. The advantages of this new methodology are: isolation of highly pure products without chromatography techniques, reusability of the catalyst using a magnet, easy workup procedure and negligible leaching of palladium.

1. Introduction

One of the significant structural motifs in organic compounds, bioactive materials, pharmaceuticals and natural products are olefins [1]. These alkene derivatives ordinarily demonstrated anti-inflammatory [2], cardioprotective [3], antitumor [4] and neuro-protective [5] properties. Due to importance of the preparation of olefins, a wide range of synthetic methods have been developed. Palladium(0) catalyzed Mizoroki-Heck cross-coupling reaction, a Nobel thought, is among the most widely used procedures for the formation of $C(sp^2)$-$C(sp^2)$ bonds in organic synthesis [6], which allows the alkylation, arylation or vinylation of numerous alkenes *via* their reaction with vinyl, aryl, benzyl or allyl halides in the presence of a base [7]. Homogeneous palladium catalysts have been widely considered in synthetic organic chemistry due to their high selectivity and catalytic activity [8]. Recycling of the catalyst, purification of the products and deactivation of the catalyst are numerous disadvantages of homogeneous catalysts. Furthermore, because of high cost and toxicity of Pd, its removal from synthetic products is highly appropriate [9]. Isolation and separation of the final products is attained by centrifugation or simple filtration when immobilized catalytically active molecule on a solid material is used. Moreover, these methods reduce heavy metal environmental contamination and barricade the loss of trace amounts of the catalysts which is beneficial in the usage of costly catalysts [10]. Although, heterogeneous catalysts can be easily recovered and reused, their active sites are not as attainable as in homogeneous catalysts, and therefore, the catalytic activity is regularly reduced. Nanocatalysts bridge the gap between heterogeneous and homogeneous catalysis, keeping the appropriate attributes of both systems [11]. Recently, in addition to classical Pd complexes [12], solid supported palladium nanoparticles has attracted great attention in provision of stable and active catalytic systems. Several supports such as silica-based and mesoporous materials [13], metal oxides [14], dendrimers [15], polymers [16], carbon nanotubes [17], ionic liquids [18], gelatin [19], polyaniline [20], carbohydrate-based materials [21] and polyvinylpyrrolidone [22] have been employed. Magnetic nanoparticles (MNPs) have attracted increasing attention in catalysis, magnetic fluids, adsorbent, biotechnology data storage, environmental remediation and biomedicine applications [23]. Magnetite (Fe_3O_4) is quite attractive due to its low-cost, unique magnetic features and strong absorption characteristics [24]; though, pure Fe_3O_4 applications are limited by its ease of oxidation, poor flame retardant effect and fast heat transfer. Several polymeric and inorganic substances have been described as carriers of magnetic materials to solve these problems

* Department of Chemistry, Faculty of Science, Arak University, 38156-88349, Arak, Iran.
E-mail addresses: mbodaghi2007@yahoo.com, m-bodaghifard@araku.ac.ir.

https://doi.org/10.1016/j.jorganchem.2019.02.010
0022-328X/

[25]. Among them, the creation core-shell nanostructures have been recognized as the most efficient method [26]. Due to non-toxicity, biocompatibility, excellent stability, and easy modification by organosilane coupling agents, the silica coating is a good surface modifier [27]. In this paper, the preparation and characterization of a novel and heterogeneous nanocatalyst was focused on, using Fe_3O_4 magnetic nanoparticles coated with SiO_2 as a convenient support for palladium with melamine as an appropriate ligand, and this reusable catalyst was applied for the Heck reaction (Scheme 1).

2. Experimental

2.1. Preparation of palladium-melamine stabilized on Fe_3O_4@SiO_2 MNPs (MNPs-Mel-Pd)

Fe_3O_4 MNPs were synthesized in alkali solution of Fe(III) and Fe(II) (2:1) at 80 °C using the chemical co-precipitation technique [28]. The Fe_3O_4 magnetic nanoparticles coated with SiO_2 were prepared using the Stober method [29]. Aminopropyl-modified silica-coated MNPs (Fe_3O_4@SiO_2-Pr-NH_2) was obtained via a described method in the literature [30]. Triazine dichloride-functionalized silica-coated MNPs (MNPs-TDCl) were synthesized according to the authors' recently reported procedure [31]. *N*-ethyldiisopropylamine, as a base (0.7 mL), was added to a mixture of the oven-dried Fe_3O_4@SiO_2-Pr-NH_2 MNPs (1 g) and dried THF (10 mL) in a 50 mL round-bottomed flask. The mixture was stirred in ice bath for 15 min at 5 °C, and then, cyanuric chloride (1 g) was added to the reaction mixture and stirred for 24 h at this temperature. The ligand grafted silica-coated MNPs were isolated by an external magnet and washed with hot THF to remove unreacted cyanuric chloride. Using an ultrasonic bath, MNPs-TDCl nanoparticles (1.0 g) were dispersed in 40 mL dioxane in a 100 mL round-bottomed flask and 15 mL ammonia (25%) was added to the suspension. The reaction mixture was refluxed at 80 °C for 24 h. The Melamine grafted on Fe_3O_4@SiO_2 MNPs (MNPs-Mel) was separated using a magnet, washed with dioxane and dried under vacuum. Palladium-melamine stabilized on Fe_3O_4@SiO_2 MNPs(MNPs-Mel-Pd) catalyst was prepared in a typical procedure as follows: MNPs-Mel (1 g) and $PdCl_2$ (0.034 g, 0.2 mmol) were stirred in DMF (5 mL) at 100 °C for 24 h. Magnetic nanocatalyst was separated with an external magnet and washed with deionized water to remove the excess $PdCl_2$ and dried under vacuum to obtain the final catalyst (MNPs-Mel-Pd) which was then used in the Heck coupling reaction.

2.2. General procedure for Heck reaction

A mixture of aryl halide (1 mmol), alkene (1.2 mmol), K_2CO_3 (2 mmol) and MNPs-Mel-Pd (0.02 g) was stirred in DMF at 100 °C and the progress of the reaction was monitored by TLC. After completion of the reaction, the catalyst was separated using an external magnet, the mixture was cooled to room temperature and the product was solidified by addition of water to the mixture and pure products were obtained in yields of 76–99%. The chromatographic techniques were not used to isolate the products.

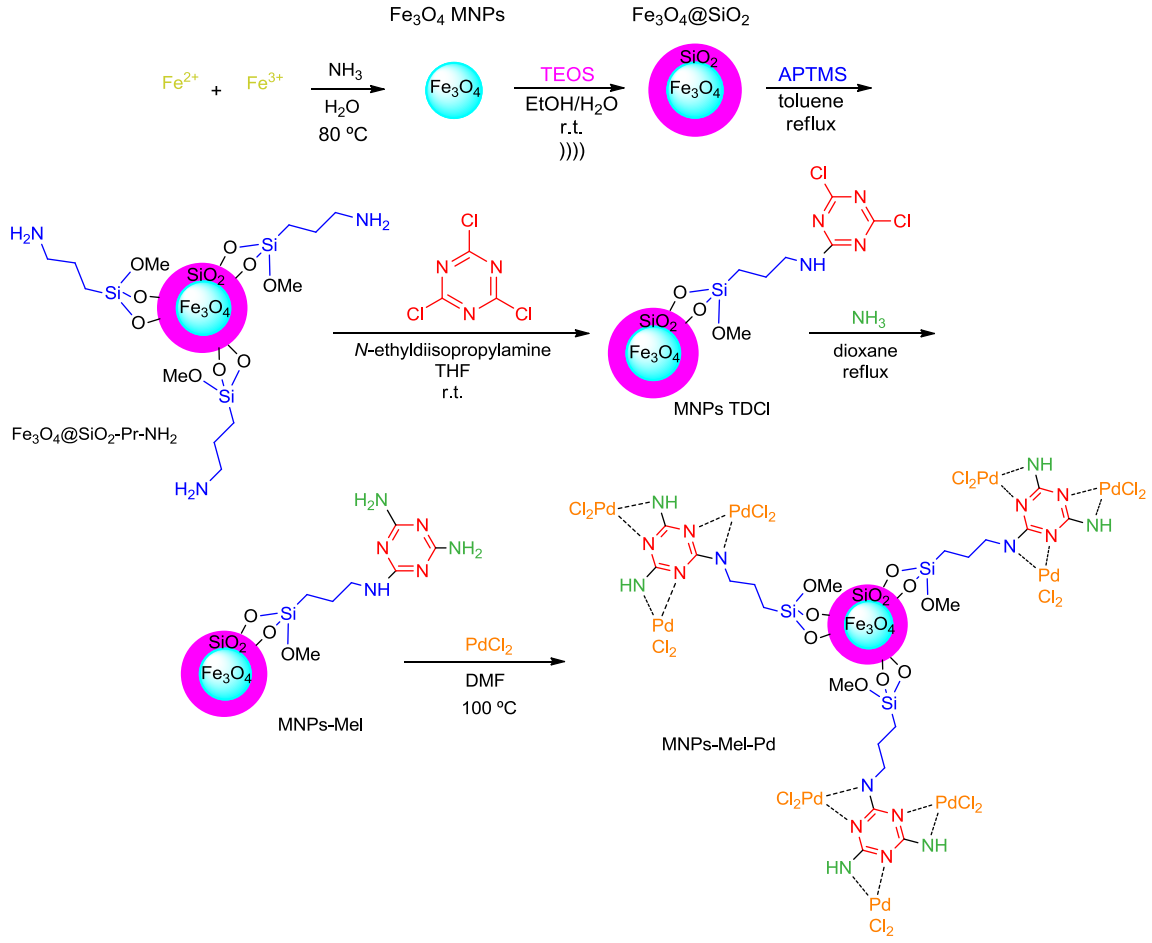

Scheme 1. Synthesis of palladium-melamine stabilized on Fe_3O_4@SiO_2 MNPs (MNPs-Mel-Pd).

3. Results and discussion

3.1. Characterization of novel MNPs-Mel-Pd catalyst

The nanocatalyst was prepared using a simple route, which is shown in Scheme 1 and was characterized using Fourier transform infrared (FT-IR) spectroscopy, scanning electron microscopy (SEM), transmission electron microscopy (TEM), X-ray diffraction (XRD), energy-dispersive X-ray spectroscopy (EDS), vibrating sample magnetometry (VSM), thermogravimetric (TGA) and ICP/OES analysis.

FT-IR spectra can be used to demonstrate successful functionalization of the MNPs. The FT-IR spectra for Fe_3O_4 nanoparticles, Fe_3O_4@SiO_2, Fe_3O_4@SiO_2-Pr-NH_2, MNPs-TDCl, MNPs-Mel and MNPs-Mel-Pd are shown in Fig. 1. The strong band at 584 cm^{-1} shows the characteristic Fe-O bonds of Fe_3O_4 (Fig. 1a). The spectrum of Fe_3O_4 shows that a band appeared at 1631 cm^{-1} corresponding to the stretching vibrational mode of H-O-H adsorbed layer. Furthermore, stretching vibration bands in the range of 3200–3500 cm^{-1} include both symmetric and asymmetric modes of O-H bonds. Fe_3O_4@SiO_2 shows characteristic FT-IR asymmetric stretching bands at 1082 cm^{-1} and symmetric stretching at 964, 806 and 457 cm^{-1} for the Si-O-Si group and supports the creation of SiO_2 shell (Fig. 1b). The immobilization of the attached alkyl groups was indicated by the weak bands at 2926 and 2972 cm^{-1} related to C-H stretching modes (Fig. 1c). In heterocyclic rings, C=C and C=N bonds are indicated by the bands at 1490-1620 cm^{-1} (Fig. 1d and e). Furthermore, the band change in the range of 1400–1650 cm^{-1} and 700 cm^{-1} of MNPs-Mel-Pd spectrum (Fig. 5f), is attributed to the formation of palladium complex [32,33]. All these bands show that the surface of the MNPs was successfully modified with grafted functional groups.

As shown in Fig. 2a, the SEM image of MNPs-Mel-Pd reveal that these nanoparticles have been formed with a mean diameter of about 20–30 nm and a spherical structure. Moreover, no significant change in the surface morphology occurred with the bonding of the palladium onto MNPs-Mel. The morphology of MNPs-Mel-Pd was studied using TEM. The dark nano Fe_3O_4 cores are surrounded by grey silica shell about 5–10 nm thick, and the mean size of the synthesized nanoparticles grain size is about 20–25 nm (Fig. 2b).

The EDS analysis of the MNPs-Mel-Pd (Fig. 3) indicates that Pd particles are loaded onto the MNPs-Mel surface. The EDS spectrum also showed characteristic signals for Fe, O, Si, C and N. The exact amount of palladium in MNPs-Mel-Pd was measured using the ICP/OES technique. Based on ICP/OES analysis, the amount of palladium in the catalyst is 1.79×10^{-3} mol g^{-1}.

Purity and crystalline nature of synthesized nano Fe_3O_4, MNPs-Mel and MNPs-Mel-Pd were investigated using XRD (Fig. 4). These diffractograms display seven characteristic Bragg's peaks appearing at $2\theta = 30.3, 35.6, 43.3, 53.8, 57.3, 62.9$ and 74.5° which correspond to the (220), (311), (400), (422), (511), (440) and (533) crystal planes of the cubic inverse spinel structured magnetite and these match well with the standard Fe_3O_4 sample (JCPDS card no. 85-1436) (Fig. 4a). The emergence of a broad hump around $2\theta = 24^\circ$ is consistent with an amorphous silica phase Fe_3O_4@SiO_2 (Fig. 4b) [34]. The presence of the new peaks at $2\theta = 40.1$, 46.9 and 69.1, which corresponding to the (111), (200) and (220) planes, are attributed to the Pd species indicating that Pd element exist in Pd^0 and Pd^{2+} forms (Fig. 4c) [34]. Similar characteristic Bragg's peaks indicate that the surface modification of the nanoparticles does not have any influence on its crystallographic phase. Besides, the Scherrer's equation that establishes a relationship between broadening and peak position has been used to estimate average crystallite size of the nanoparticles using the peak of highest intensity, that is, the (311) peak in this case and it has been calculated to be 20.1 nm [35], which is in the range of the size determined by FE-SEM and TEM analysis (Fig. 2).

The functionalization of Fe_3O_4 MNPs with organic layers and Melamine complex of palladium and its stability is inferred using thermogravimetric analysis (TGA) and derivative thermogravimetry (DTG) (Fig. 5). The weight loss at temperatures below 200 °C (4%) is due to the removal of physically adsorbed solvent and surface hydroxyl groups on the catalyst support. The organic fractions are decomposed in the range of 200–580 °C. The main weight loss of the organic grafting is about 17%, which is similar to the elemental analysis, and obvious thermal degradation occurs at 220 °C, which reveals acceptable stability. According to this weight loss, 0.57 mmol of organic compounds were loaded on 1 gr of MNPs-Mel-Pd.

The magnetic properties of nanoparticles were characterized

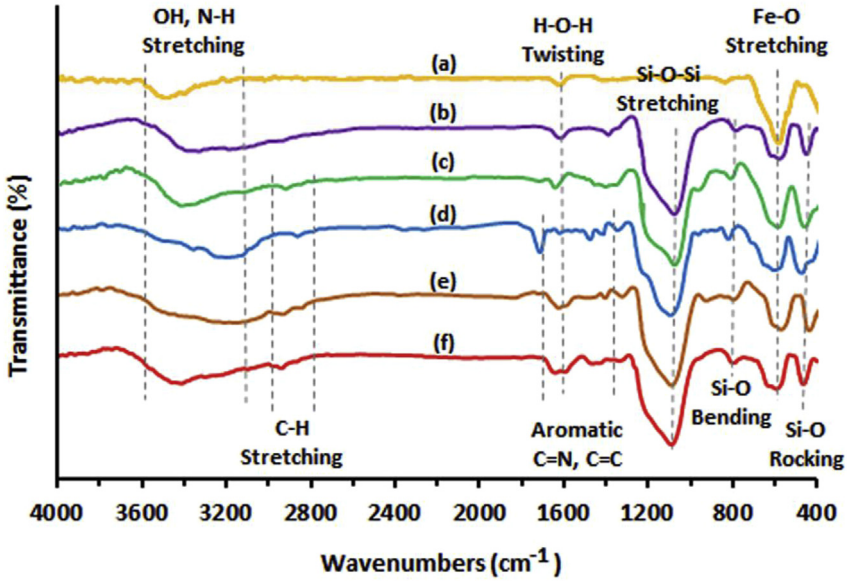

Fig. 1. FT-IR spectra of (a) Fe_3O_4 MNPs, (b) Fe_3O_4@SiO_2, (c) Fe_3O_4@SiO_2-Pr-NH_2, (d) MNPs-TDCl, (e) MNPs-Mel and (f) MNPs-Mel-Pd.

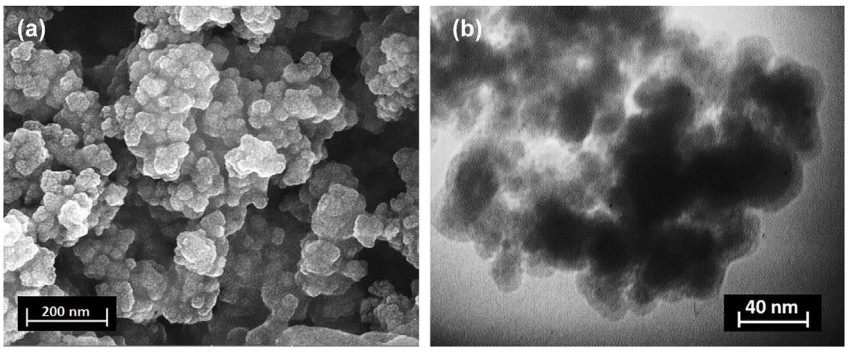

Fig. 2. (a) FE-SEM image and (b) TEM image of MNPs-Mel-Pd nanoparticles.

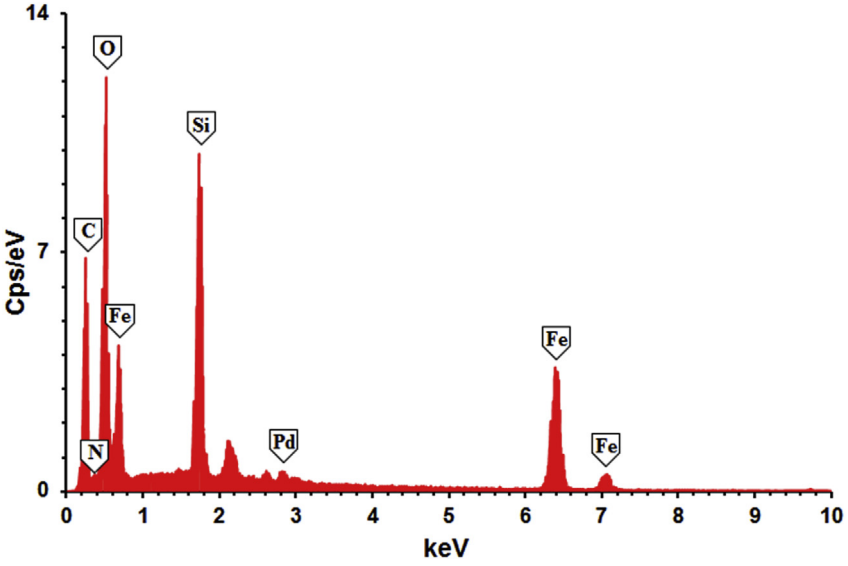

Fig. 3. EDS spectrum of MNPs-Mel-Pd.

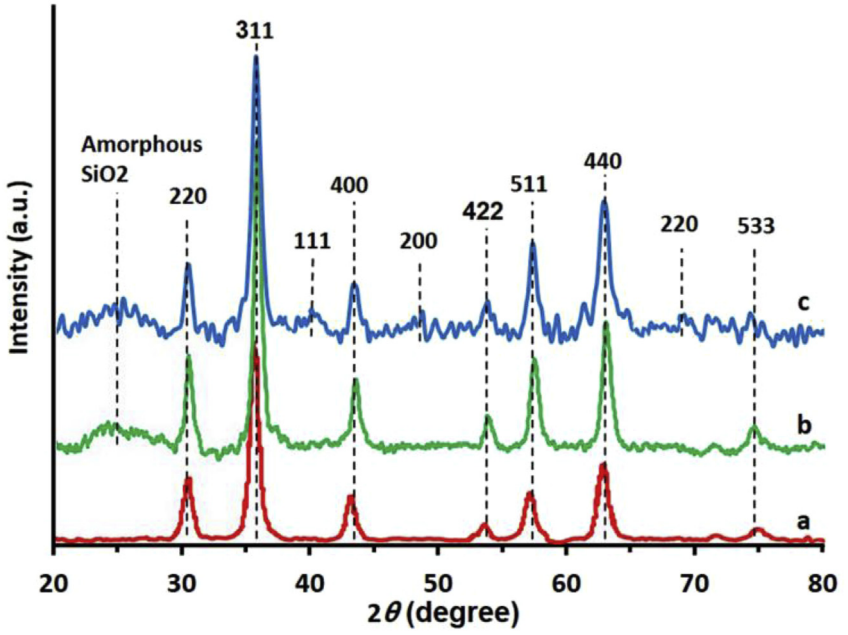

Fig. 4. XRD diffraction pattern of (a) Fe_3O_4 MNPs (b) MNPs-Mel and (C) MNPs-Mel-Pd.

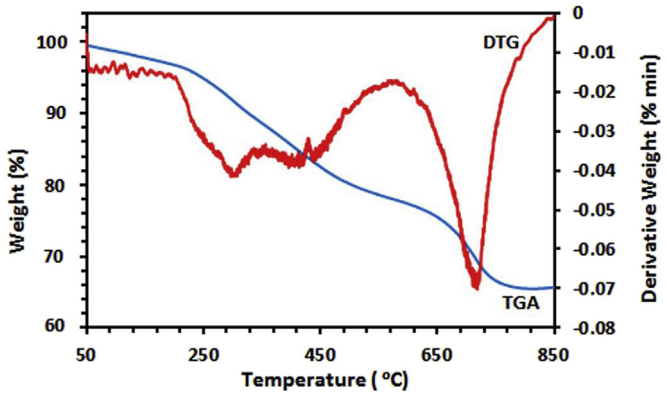

Fig. 5. TG-DTG analyses for MNPs-Mel-Pd.

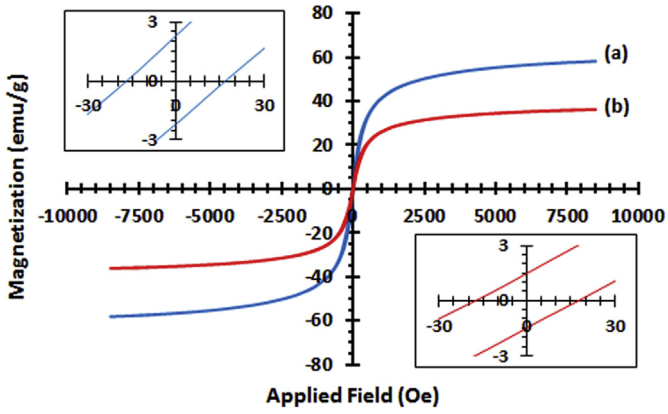

Fig. 6. Magnetic hysteresis loops of (a) Fe_3O_4 MNPs and (b) MNPs-Mel-Pd.

using vibrating sample magnetometer (VSM). Fig. 6 shows the typical room temperature magnetization (*M*) *versus* magnetic field (*H*) (*M-H* curves or hysteresis loops) of Fe_3O_4 MNPs and MNPs-Mel-Pd. The nanoparticles display a typical superparamagnetic behavior. The saturation magnetization of the Fe_3O_4 MNPs (Fig. 6a) is 57.9 emu/g, which is lower than its bulk counter parts (92.0 emu/g) [36]. The saturation magnetization of MNPs-Mel-Pd was 35.8 emu/g, which is lower than that of Fe_3O_4 MNPs (Fig. 6b). This might be due to the creation of a silica shell and organic shell around the Fe_3O_4 core.

3.2. Catalytic study

After characterization of the MNPs-Mel-Pd catalyst, its catalytic activity was evaluated in C-C coupling Heck reaction (Scheme 2).

Firstly, using iodobenzene and styrene, a model reaction was selected to optimize carbon-carbon coupling bond formation in

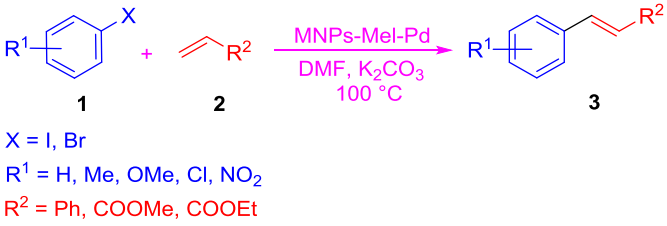

Scheme 2. MNPs-Mel-Pd catalyzed Heck reaction.

Table 1
Optimization of reaction conditions for C-C coupling reaction.[a]

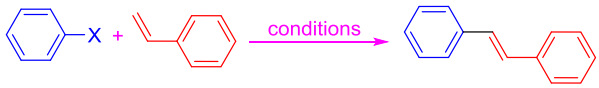

Entry	Solvent	Base	catalyst (mg)	Temp. (°C)	Yield (%)[b]
1	Toluene	K_2CO_3	MNPs-TDA-Pd (20)	100	17
2	DMSO	K_2CO_3	MNPs-TDA-Pd (20)	100	45
3	EtOH	K_2CO_3	MNPs-TDA-Pd (20)	reflux	23
4	H_2O	K_2CO_3	MNPs-TDA-Pd (20)	reflux	0
5	DMF	K_2CO_3	MNPs-TDA-Pd (20)	100	93
6	DMF	Et_3N	MNPs-TDA-Pd (20)	100	52
7	DMF	KOH	MNPs-TDA-Pd (20)	100	56
8	DMF	Na_2CO_3	MNPs-TDA-Pd (20)	100	47
9	DMF	–	MNPs-TDA-Pd (20)	100	0
10	DMF	K_2CO_3	MNPs-TDA-Pd (20)	80	77
11	DMF	K_2CO_3	MNPs-TDA-Pd (20)	60	51
12	DMF	K_2CO_3	MNPs-TDA-Pd (20)	120	75
13	DMF	K_2CO_3	MNPs-TDA-Pd (40)	100	89
14	DMF	K_2CO_3	MNPs-TDA-Pd (10)	100	72
15	DMF	K_2CO_3	–	100	–
16	DMF	K_2CO_3	Fe_3O_4 (20)	100	–
17	DMF	K_2CO_3	Fe_3O_4@SiO_2 (20)	100	–
18	DMF	K_2CO_3	Fe_3O_4@SiO_2-Pr-NH_2 (20)	100	–
19	DMF	K_2CO_3	Fe_3O_4@SiO_2-TDCl (20)	100	–
20	DMF	K_2CO_3	Fe_3O_4@SiO_2-Mel (20)	100	–

[a] Reaction conditions: iodobenzene (1 mmol), styrene (1.2 mmol), base (2 mmol), 8 h.
[b] Isolated yield.

Table 2
Diversity of Heck reaction using MNPs-Mel-Pd under optimal conditions.[a]

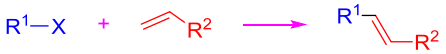

Entry	R^1	R^2	X	Yield (%)[b]
1	2,4,6-$(Cl)_3C_6H_2$	CO_2Me	I	86
2	2,4-$(Cl)_2C_6H_3$	CO_2Me	I	84
3	C_6H_5	CO_2Me	I	96
4	C_6H_5	CO_2Me	Br	88
5	4-$OMeC_6H_4$	CO_2Me	I	88
6	4-$NO_2C_6H_4$	CO_2Me	I	99
7	4-$NO_2C_6H_4$	CO_2Me	Br	91
8	2-$NO_2C_6H_4$	CO_2Me	I	85
9	4-ClC_6H_4	CO_2Me	I	92
10	4-ClC_6H_4	CO_2Me	Br	80
11	4-MeC_6H_4	CO_2Me	I	89
12	C_6H_5	CO_2Et	I	90
13	C_6H_5	CO_2Et	Br	81
14	4-$OMeC_6H_4$	CO_2Et	I	87
16	4-$NO_2C_6H_4$	CO_2Et	I	97
17	4-$NO_2C_6H_4$	CO_2Et	Br	86
18	2-$NO_2C_6H_4$	CO_2Et	I	79
19	4-ClC_6H_4	CO_2Et	I	90
20	4-ClC_6H_4	CO_2Et	Br	84
21	4-MeC_6H_4	CO_2Et	I	89
22	C_6H_5	Ph	I	93
23	C_6H_5	Ph	I	93
24	4-$OMeC_6H_4$	Ph	I	76
25	4-$NO_2C_6H_4$	Ph	I	95
26	4-$NO_2C_6H_4$	Ph	Br	86
27	2-$NO_2C_6H_4$	Ph	I	83
28	4-ClC_6H_4	Ph	I	91
29	4-ClC_6H_4	Ph	Br	83
30	4-MeC_6H_4	Ph	I	88

[a] Reaction conditions: iodobenzene (1 mmol), styrene (1.2 mmol), base (2 mmol), MNPs-Mel-Pd (0.02 g), DMF, 8 h, 100 °C.
[b] Isolated yield.

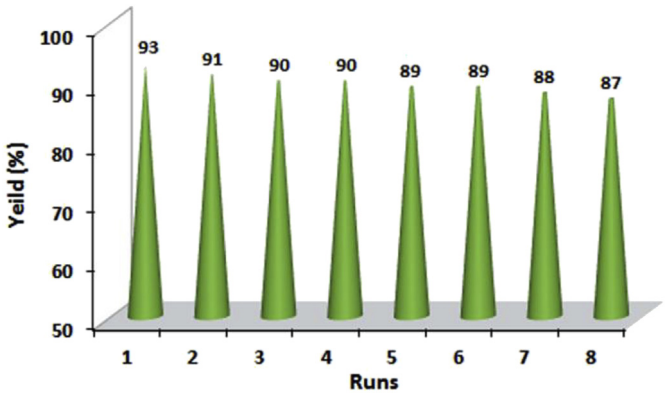

Fig. 7. Recyclability of catalyst in the coupling reaction of iodobenzene and styrene {Condition: MNPs-TDA-Pd (20 mg), K_2CO_3 (2 mmol), DMF, 100 °C, 8 h}.

the presence of MNPs-Mel-Pd as an effective and magnetically separable nanocatalyst. To provide appropriate reaction media, several solvents such as toluene, DMSO, EtOH, H_2O, DMF and water were examined. It was shown that DMF provided the best yield of the desired product (Table 1, entries 1-5). Afterwards, the effect of the base on the yield of the Heck reaction was examined and it was found that K_2CO_3 gave a better result than Et_3N, KOH and Na_2CO_3 (Table 1, entries 6-9). In order to increase the product yield and reduce the reaction time, the model reaction was tested at various temperatures, and at 100 °C, a marked increase in the reaction yield and decrease in reaction time was observed (Table 1, entries 10-12). Comparable yields were obtained when the activity of the nanocatalyst in numerous amounts was tested. The best result was obtained with 20 mg of MNPs-Mel-Pd and in the absence of the nanocatalyst, no product was formed (Table 1, entries 13-20).

Under the optimized reaction conditions, the scope of catalytic efficacy of the MNPs-Mel-Pd catalyst in Heck reaction was extended to the various electron-releasing and electron-withdrawing aryl iodides and bromides with styrene, methyl and ethyl acrylate (Table 2). As shown in Table 2, in the efficient coupling reactions of aryl iodides bearing electron-donating or -withdrawing substituents with olefins at 100 °C for 8 h, products in good to excellent yields (76–99%) were obtained. Also, the MNPs-Mel-Pd catalyst displayed good activity towards bromobenzene with electron-withdrawing aryl bromides and acceptable yields (80-91%) were obtained when the Heck coupling reactions was carried out at 100 °C for 8 h. In general, methyl and ethyl acrylate are more active than styrene and a substituent such as nitro at the *ortho* position of aryl halides slightly reduces the yield of the desired product due to its steric effect. The product yield for the aryl iodides are higher than aryl bromides, and the product yields for the aryl halides with electron-withdrawing groups were higher than that with electron-donating groups. As a result, it is concluded that the MNPs-Mel-Pd is an effective catalyst for Heck reaction and also displays wide range of functional group tolerance.

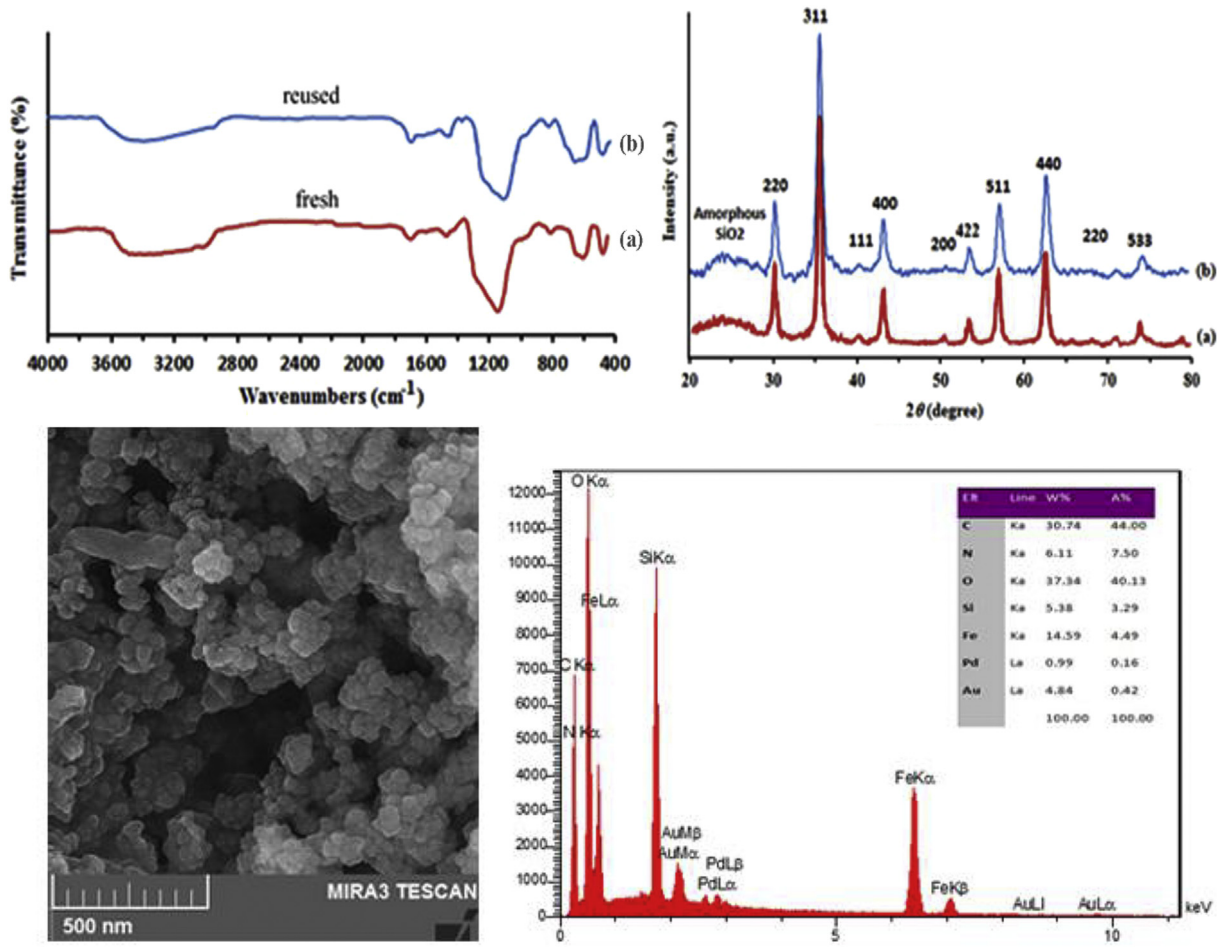

Fig. 8. The FT-IR spectra and SEM image (left), and the XRD diffraction patterns and EDS analysis of catalyst (right); {fresh catalyst (a) and eight times reused catalyst (b)}.

Table 3
Comparison of results for MNPs-Mel-Pd with those for other catalysts in the coupling of iodobenzene with styrene.

Entry	Catalyst (mol% of Pd)	Conditions	Yield (%)[a]
1	Pd/MFC (30 mg, Pd: 0.308 mol %)	K_2CO_3, DMF, 120 °C, 1 h	66 [37]
2	Fe_3O_4/SiO_2/HPG-$OPPh_2$-PNP (1.14 mol% of Pd)	K_2CO_3, DMF, 100 °C, 1 h	87 [14a]
3	$Fe_3O_4/SiO_2/NH_2$-Pd (30 mg)	NaOAc, CH_3CN/H_2O, reflux, 12 h	71 [38]
4	$[Pd(NH_3)_4]^{2+}$-NaY (0.1 mol % Pd)	NaOAc, DMF, 140 °C, 20 h	85 [39]
5	$[MePPh_3]_2[Pd_2Br_2Cl_4]$ (0.04 mmol)	$NaHCO_3$, DMF, 140 °C, 12 h	58 [40]
6	Pd/Fe_3O_4@C (30 mg, Pd: 0.308 mol %)	K_2CO_3, DMF, 120 °C, 2 h	66 [37]
7	palladium supported/PAEIP (30 mg)	Et_3N, Dioxane, 100 °C, 24 h	84 [41]
8	Pd-LHMS-3 (50 mg Pd)	triethanolamine, 100 °C, reflux, 10 h	85 [42]
9	MNPs-TDA-Pd (20 mg)	K_2CO_3, DMF, 100 °C, 8 h	93 This work

[a] Isolated yield.

It is reasonable to believe that the Pd grafting with organic functional groups on inorganic support efficiently limit Pd leaching and particle growth, which permitted this hybrid nanocatalyst to be reused several times with only a slight loss of its activity. Clearly, the functionalized catalysts were more stable than the non-functionalized catalysts, which lost their activity gradually because of metal leaching and Pd particle growth.

3.3. Reusability of catalyst and heterogeneity test

Recovery of the palladium catalyst at the termination of the reaction is the essential part of the Heck coupling reaction. Therefore, the reusability and recovery of MNPs-Mel-Pd catalyst was examined in the reaction of iodobenzene and styrene under the optimized condition. After completion of the reaction, the catalyst was collected by an external magnet, washed with ethanol several times, dried under vacuum and reused for the next run. The recycled MNPs-Mel-Pd catalyst was reused eight times with little loss of activity (Fig. 7).

Heterogeneity and palladium leaching of this hybrid nanocatalyst for the model Heck reaction were examined by the modified 'hot filtration' test. The reaction was stopped at 50% conversion. The solid nanocatalyst was deposited on the magnetic bar. Half of the liquid reaction mixture was placed into another reaction tube. After an additional 1 h heating at 100 °C, the catalyst-free portion showed no additional conversion, evidently proving the heterogeneity of catalyst.

Potential Pd leaching into the reaction mixture was also analyzed with ICP/OES analysis after eight runs. The amount of palladium in the catalyst is found to be 1.73×10^{-3} mol g^{-1} after eight cycles based on ICP/OES measurements. The palladium content in MNPs-Mel-Pd after six runs is comparable to that of fresh catalyst (1.79×10^{-3} mol g^{-1} for fresh MNPs-Mel-Pd), confirming that the leaching of palladium in the reaction mixture is negligible.

Also it is apparent from comparison of the FT-IR spectrum, XRD diffraction patterns, SEM image and EDS analysis of the reused catalyst (MNPs-Mel-Pd), after eight runs, the recovered catalyst had no understandable variation in structure and morphology (Fig. 8). Therefore, these studies suggesting that the prepared hybrid nanocatalyst possessed good reusability and stability.

3.4. Comparison of catalyst

In order to examine the efficiency of the present procedure in comparison with previously reported protocols, the results of the Heck coupling reaction of iodobenzene with styrene in the presence of other Pd catalysts were compared. As shown in Table 3, in contrast to previously reported systems, the catalytic system in this project does not suffer from the harsh reaction conditions such as high temperature, high amount of catalyst and long reaction time. In addition, the recyclability and recoverability of this nanocatalyst are more quick and easier than those of the other catalysts. Furthermore, the Palladium leaching is negligible.

4. Conclusions

In this work, a palladium-melamine complex stabilized on Fe_3O_4@SiO_2 MNPs (MNPs-Mel-Pd) catalyst was prepared, which displays superb catalytic efficiency towards Heck reaction. The synthesized catalyst was confirmed by FT-IR, XRD, TGA, ICP/OES, VSM, TEM, FE-SEM and EDS techniques. The efficiency of the nanocatalyst was tested in Heck reaction for preparation of target products in good to excellent yields under moderate to mild experimental conditions. The good catalytic activity after eight runs due to the negligible leaching of palladium (analyzed by ICP/OES technique) from the support during the reaction, confirming high stability of the catalyst. This reported method offers numerous significant advantages such as isolation of highly pure products without chromatography technique, simple product separation procedure, reusability of the catalyst using a magnet and reuse without loss of its catalytic activity.

Acknowledgements

The authors gratefully acknowledge the financial support of this work by the Research Council of Arak University.

Appendix A. Supplementary data

Supplementary data to this article can be found online at https://doi.org/10.1016/j.jorganchem.2019.02.010.

References

[1] a) A.B. Dounay, L.E. Overman, Chem. Rev. 103 (2003) 2945;
b) K. Nicolaou, P.G. Bulger, D. Sarlah, Angew. Chem. Int. Ed. 44 (2005) 4442.
[2] N. Elmali, O. Baysal, A. Harma, I. Esenkaya, B. Mizrak, Inflammation 30 (2007) 1;
[3] N. Gurusamy, I. Lekli, S. Mukherjee, D. Ray, M.K. Ahsan, M. Gherghiceanu, L.M. Popescu, D.K. Das, Cardiovasc. Res. (2009) cvp384.
[4] M. Jang, L. Cai, G.O. Udeani, K.V. Slowing, C.F. Thomas, C.W. Beecher, H.H. Fong, N.R. Farnsworth, A.D. Kinghorn, R.G. Mehta, Science 275 (1997) 218.
[5] S.S. Karuppagounder, J.T. Pinto, H. Xu, H.-L. Chen, M.F. Beal, G.E. Gibson, Neurochem. Int. 54 (2009) 111.
[6] a) R.F. Heck, Palladium Reagents in Organic Syntheses, Academic Press, New York, 1985;
b) R.F. Heck, J. Nolley Jr., J. Org. Chem. 37 (1972) 2320.
[7] a) M. Oestreich, The Mizoroki-Heck Reaction, John Wiley, New York, 2009;
b) V. Polshettiwar, C. Len, A. Fihri, Coord. Chem. Rev. 253 (2009) 2599;
c) G. Meng, M. Szostak, Angew. Chem. Int. Ed. 54 (2015) 14518;
d) Ch Liu, G. Meng, M. Szostak, J. Org. Chem. 81 (2016) 12023.
[8] G. Hervé, G. Sartori, G. Enderlin, G. Mackenzie, C. Len, RSC Adv. 4 (2014) 18558.
[9] a) V. Polshettiwar, R. Luque, A. Fihri, H. Zhu, M. Bouhrara, J.-M. Basset, Chem. Rev. 111 (2011) 3036;
b) C.W. Lim, I.S. Lee, Nano Today 5 (2010) 412.
[10] B. Karimi, F. Mansouri, H.M. Mirzaei, ChemCatChem 7 (2015) 1736.

[11] a) R.B.N. Baig, R.S. Varma, Chem. Commun. 49 (2013) 752;
b) D. Zhang, C. Zhou, Z. Sun, L.-Z. Wu, C.-H. Tung, T. Zhang, Nanoscale 4 (2012) 6244.
[12] a) B. Agrahari, S. Layeka, Anuradhaa, R. Ganguly, D.D. Pathak, Inorg. Chim. Acta 471 (2018) 345;
b) S. Layek, Anuradha, B. Agrahari, D.D. Pathak, J. Organomet. Chem. 846 (2017) 105.
[13] a) J. Demel, S.-E. Park, J. Čejka, P. Štěpnička, Catal. Today 132 (2008) 63;
b) A. Barau, V. Budarin, A. Caragheorgheopol, R. Luque, D.J. Macquarrie, A. Prelle, V.S. Teodorescu, M. Zaharescu, Catal. Lett. 124 (2008) 204;
c) M. Azaroon, A.R. Kiasat, Appl. Organomet. Chem. (2018) e4271;
d) M. Luo, Ch Dai, Q. Han, G. Fan, G. Song, Surf. Interface Anal. 48 (2016) 1066;
e) S.F. Motevalizadeh, M. Alipour, F. Ashori, A. Samzadeh-Kermani, H. Hamadi, M.R. Ganjali, H. Aghahosseini, A. Ramazani, M. Khoobi, E. Gholibegloo, Appl. Organomet. Chem. 32 (2018) e4123;
f) S. Sobhani, F. Zarifi, Chin. J. Catal. 36 (2015) 555.
[14] a) Q. Du, W. Zhang, H. Ma, J. Zheng, B. Zhou, Y. Li, Tetrahedron 68 (2012) 3577;
b) M. Ma, Q. Zhang, D. Yin, J. Dou, H. Zhang, H. Xu, Catal. Commun. 17 (2012) 168;
c) K. Bahrami, M.M. Khodaei, F.S. Meibodi, Appl. Organomet. Chem. 31 (2017) e3627;
d) K.-M. Choi, T. Mizugaki, K. Ebitani, K. Kaneda, Chem. Lett. 32 (2003) 180.
[15] K.R. Gopidas, J.K. Whitesell, M.A. Fox, Nano Lett. 3 (2003) 1757.
[16] B. Tamami, S. Ghasemi, J. Mol. Catal. 322 (2010) 98.
[17] a) M.R. Nabid, Y. Bide, S.J.T. Rezaei, Appl. Catal. Gen. 406 (2011) 124;
b) A. Corma, H. Garcia, A. Leyva, J. Mol. Catal. Chem. 230 (2005) 97.
[18] a) V. Calò, A. Nacci, A. Monopoli, P. Cotugno, Angew. Chem. Int. Ed. 121 (2009) 6217;
b) Z. Zhang, Z. Zha, C. Gan, C. Pan, Y. Zhou, Z. Wang, M.-M. Zhou, J. Org. Chem. 71 (2006) 4339.
[19] H. Firouzabadi, N. Iranpoor, A. Ghaderi, J. Mol. Catal. Chem. 347 (2011) 38.
[20] A. Houdayer, R. Schneider, D. Billaud, J. Ghanbaja, J. Lambert, Appl. Organomet. Chem. 19 (2005) 1239.
[21] a) A. Khalafi-Nezhad, F. Panahi, Green Chem. 13 (2011) 2408;
b) H. Firouzabadi, N. Iranpoor, F. Kazemi, M. Gholinejad, J. Mol. Catal. Chem. 357 (2012) 154;
c) S. Kumari Anuradha, S. Layek, D.D. Pathak, New J. Chem. 41 (2017) 5595.
[22] a) C. Evangelisti, N. Panziera, P. Pertici, G. Vitulli, P. Salvadori, C. Battocchio, G. Polzonetti, J. Catal. 262 (2009) 287;
b) R.P. Jumde, M. Marelli, N. Scotti, A. Mandoli, R. Psaro, C. Evangelisti, J. Mol. Catal. Chem. 414 (2016) 55.
[23] a) L. Wu, A. Mendoza-Garcia, Q. Li, S. Sun, Chem. Rev. 116 (2016) 10473;
b) S.C. Tang, I.M. Lo, Water Res. 47 (2013) 2613;
c) U. Häfeli, W. Schütt, J. Teller, M. Zborowski, Scientific and Clinical Applications of Magnetic Carriers, Springer Science & Business Media, Berlin, 2013.
[24] a) R. Zhao, K. Jia, J.-J. Wei, J.-X. Pu, X.-B. Liu, Mater. Lett. 64 (2010) 457;
b) A. Ghorbani-Choghamarani, B. Tahmasbi, P. Moradi, Appl. Organomet. Chem. 30 (2016) 422.
[25] A. Schätz, O. Reiser, W.J. Stark, Chem. Eur J. 16 (2010) 8950.
[26] a) M.A. Bodaghifard, S. Asadbegi, Z. Bahrami, J. Iran. Chem. Soc. 14 (2017) 365;
b) H. Moghanian, A. Mobinikhaledi, A. Blackman, E. Sarough-Farahani, RSC Adv. 4 (2014) 28176;
c) Q. Zhang, X. Zhao, H.-X. Wei, J.-H. Li, J. Luo, Appl. Organomet. Chem. 31 (2017) e3608.
[27] Y. Piao, A. Burns, J. Kim, U. Wiesner, T. Hyeon, Adv. Funct. Mater. 18 (2008) 3745.
[28] K. Can, M. Ozmen, M. Ersoz, Colloids Surf., B 71 (2009) 154.
[29] W. Stöber, A. Fink, E. Bohn, J. Colloid Interface Sci. 26 (1968) 62.
[30] T. Zeng, L. Yang, R. Hudson, G. Song, A.R. Moores, C.-J. Li, Org. Lett. 13 (2011) 442;
[31] M. Bodaghifard, A. Mobinikhaledi, S. Asadbegi, Appl. Organomet. Chem. 31 (2017) e3557.
[32] C. Gomez-Vaamonde, A. Alvarez-Valdrs, M. del C. Navarro-Ranninger, J.R. Masaguer, Transition Met. Chem. 9 (1984) 52.
[33] a) P. Hu, Y. Dong, X. Wu, Y. Wei, Front. Chem. Sci. Eng. 10 (2016) 389;
b) S.A. Al-Jibori, Q.K.A. Al-Jibori, H. Schmidt, K. Merzweiler, Ch Wagner, G. Hogarth, Inorg. Chim. Acta 402 (2013) 69.
[34] a) G. Feng, D. Hu, L. Yang, Y. Cui, X.-a. Cui, H. Li, Separ. Purif. Technol. 74 (2010) 253;
b) Q. Zhao, Y. Zhu, Z. Sun, Y. Li, G. Zhang, F. Zhang, X. Fan, J. Mater. Chem. 3 (2015) 2609.
[35] J. Giri, S.G. Thakurta, J. Bellare, A.K. Nigam, D. Bahadur, J. Magn. Magn Mater. 293 (2005) 62.
[36] V.S. Zaitsev, D.S. Filimonov, I.A. Presnyakov, R.J. Gambino, B. Chu, J. Colloid Interface Sci. 212 (1999) 49.
[37] M. Zhu, G. Diao, J. Phys. Chem. C 115 (2011) 24743.
[38] Z. Wang, P. Xiao, B. Shen, N. He, Colloids Surf., A 276 (2006) 116.
[39] L. Djakovitch, K. Koehler, J. Am. Chem. Soc. 123 (2001) 5990.
[40] A.R. Hajipour, G. Azizi, Synlett 24 (2013) 254.
[41] H. Mahdavi, A. Zirakzadeh, J. Amani, React. Funct. Polym. 67 (2007) 716.
[42] A. Modak, J. Mondal, V.K. Aswal, A. Bhaumik, J. Mater. Chem. 20 (2010) 8099.